Chemical Science

ROYAL SOCIETY OF CHEMISTRY

PERSPECTIVE

View Article Online
View Journal | View Issue

Cite this: *Chem. Sci.*, 2024, **15**, 6994

All publication charges for this article have been paid for by the Royal Society of Chemistry

Received 27th March 2024
Accepted 19th April 2024

DOI: 10.1039/d4sc02028f

rsc.li/chemical-science

Contracted porphyrins and calixpyrroles: synthetic challenges and ring-contraction effects

Keita Watanabe,[a] Narendra Nath Pati [b] and Yasuhide Inokuma *[ab]

Ring-contracted porphyrin analogues, such as subporphyrins and calix[3]pyrroles, have recently attracted considerable attention not only as challenging synthetic targets but also as functional macrocyclic compounds. Although canonical porphyrins and calix[4]pyrrole are selectively generated *via* acid-catalyzed condensation reactions of pyrrole monomers, their tripyrrolic analogues are always missing under similar conditions. Recent progress in synthesis has shown that strain-controlled approaches using boron(III)-templating, core-modification, or ring tightening provide access to various contracted porphyrins. The tripyrrolic macrocycles are a new class of functional macrocycles exhibiting unique ring-contraction effects, including strong boron chelation and strain-induced ring expansion. This Perspective reviews recent advances in synthetic strategies and the novel ring-contraction effects of subporphyrins, triphyrins(2.1.1), calix[3]pyrroles, and their analogous.

1. Introduction

Intrigued by elaborate biomolecular systems such as photosynthesis[1] and oxygen delivery,[2] chemists have explored the chemistry of the porphyrins that play key roles. In recent decades, research on the synthesis of porphyrin-related compounds has been directed toward the synthesis of artificial chromophores essential to the development of organic functional materials, including photovoltaic materials,[3–7] catalysts,[8–10] and molecular machines,[11] rather than the total

[a]*Division of Applied Chemistry, Faculty of Engineering, Hokkaido University, Kita 13, Nishi 8 Kita-ku, Sapporo, Hokkaido 060-8628, Japan. E-mail: inokuma@eng.hokudai.ac.jp*

[b]*Institute for Chemical Reaction Design and Discovery (WPI-ICReDD), Hokkaido University, Kita 21, Nishi 10, Kita-ku, Sapporo, Hokkaido 001-0021, Japan*

From left to right: **Keita Watanabe**, **Narendra Nath Pati**, **and Yasuhide Inokuma**

Keita Watanabe (left) received his BS from Hokkaido University, Japan, in 2022. He is now an MC student under the supervision of Prof. Inokuma at Hokkaido University studying the chemistry of calix[3]pyrroles and related macrocycles. Narendra Nath Pati (center) received his M.Sc. from Banaras Hindu University, India, and PhD from the School of Chemistry, University of Hyderabad, India, under the supervision of Prof. Pradeepta K. Panda. Subsequently, he pursued postdoctoral research under the supervision of Prof. Pradeepta K. Panda at the same university, initially at the School of Chemistry and later at the Advanced Centre of Research in High Energy Materials. After that, he spent a year as a senior scientist in the pharmaceutical sector. He is currently a postdoctoral fellow working under Prof. Y. Inokuma at the Institute for Chemical Reaction Design and Discovery (ICReDD), Hokkaido University. His research focuses on the synthesis and application of contracted and unsymmetrical substituted porphyrionoids. Yasuhide Inokuma (right) is a Professor in the Faculty of Engineering at Hokkaido University and Principal Investigator at ICReDD. He received his PhD from Kyoto University in 2009 under the supervision of Prof. Atsuhiro Osuka. Subsequently, he worked with Prof. Makoto Fujita at the University of Tokyo as an assistant professor from 2009 and as a lecturer from 2014. In 2016, he moved to Hokkaido University, where he started his independent research and was promoted to full professor in 2023. His research interests are focused on the synthesis and applications of discrete polyketone-related molecules, including contracted porphyrinoids such as calix[3]pyrroles.

synthesis of naturally occurring molecules such as vitamin B_{12}.[12] Although enzyme-based biosynthesis has always been used by bacteria, plants, and animals, the chemical synthesis of porphyrins originates in the discovery of an acid-catalyzed condensation between pyrrole and aldehyde by Rothemund in 1935.[13] Canonical porphyrins are formed through the oxidation of porphyrinogen intermediates, which are produced through the cyclotetramerization of pyrrole monomers with four *meso*-sp^3-carbon bridges. When macrocyclization occurs with fewer or more than four pyrrole units, contracted or expanded porphyrins are formed. The discovery of sapphyrin by Woodward[14] has triggered the development of expanded porphyrins, which exhibit unique structural and optical properties derived from their enlarged inner cavity and π-conjugation.[15–17] To date, giant macrocycles with more than 20 pyrrole units have also been developed using Rothemund-type condensation of oligopyrrole precursors.[18,19] Despite the considerable development of expanded porphyrin chemistry over the last half century, research on contracted porphyrins is still in its infancy owing to the difficulty of synthesis.

Macrocyclic compounds, including calixarenes,[20] cyclodextrins,[21] and cucurbiturils,[22] as well as porphyrins, have optimal and marginal sizes that can be accessed through monomer oligomerization and subsequent macrocyclization. These sizes are typically determined by the balance between enthalpy and entropy factors. The formation of a macrocycle smaller than the optimal size is entropically favorable, although it often requires countering the enthalpy factors arising from steric repulsion and ring strain. Therefore, the synthesis of ever-smaller links in each macrocyclic family requires unconventional and well-designed methods.[23–25]

Under Rothemund- and modified Rothemund–Lindsey-type conditions, porphyrins are considered the optimal and marginal size of macrocycles composed of repeats of alternating pyrrole and methine carbon units owing to the absence of subporphyrin in the reaction mixture (Fig. 1). Subporphyrin is a contracted porphyrin composed of three pyrrole units bridged by three sp^2-hybridized carbon atoms, also known as triphyrin(1.1.1). Until the first synthesis of tribenzosubporphine by Osuka and coworkers in 2006,[26] it was unclear whether this type of macrocycle could be synthesized or even existed. This situation is in striking contrast to the fact that subphthalocyanines,[27–29] contracted phthalocyanine analogues, have been extensively developed since their first discovery by Meller and Ossko in 1972.[30] The emergence of the contracted analogues in the porphyrinoid family has, however, led to the development of synthetic methodologies and discovery of their properties.

Recent advances in the synthesis of boron-free subporphyrins[31] and calix[3]pyrrole,[32] a porphyrinogen-like analogue of subporphyrins, have expanded the potential of contracted porphyrins. Calix[4]pyrroles, tetrapyrrolic counterparts of calix[3]pyrrole, have demonstrated their distinctive supramolecular chemistry owing to the conformational diversity and molecular recognition abilities.[33,34] These properties have led to the development of a number of applications, including ion sensors,[35] selective ion bindings,[36] exchanges,[37] transporters[38] and anti-cancer drugs.[39] Since calix[4]pyrrole is the optimal and marginal size in acid-catalyzed condensation of pyrrole and acetone, similar to the porphyrin synthesis, calix[3]pyrrole has long been inaccessible by conventional methods. The synthetic breakthrough of calix[3]pyrrole has also triggered the discovery of its unique properties derived from the ring-contraction effects. This perspective introduces the recent progress in the synthesis of various ring-contracted porphyrinoids, such as triphyrin(*n*.1.1), core-modified subporphyrins, and calix[3]pyrrole analogues, according to the three typical classifications of methodology. Their structural, optical, and chemical properties are also discussed in terms of ring-contraction effects derived from the tripyrrolic ring systems. In the case of calix[3]pyrrole ring systems, their ring strain has recently been recognized as a key factor of unusual reactivity and synthetic feasibility. We also discuss our future perspective on the chemistry of contracted porphyrins and related macrocycles.

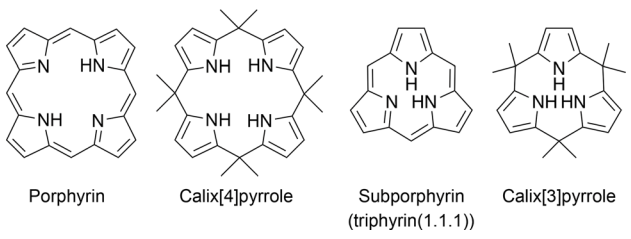

Fig. 1 Canonical porphyrin and calix[4]pyrrole accessible by acid-catalyzed pyrrole monomer condensation and their contracted analogues, subporphyrin (also known as triphyrin(1.1.1)) and calix[3]pyrrole.

2. Synthetic approaches

Rothemund–Lindsey-type direct macrocyclization of pyrrole monomers has been unsuccessful in the synthesis of subporphyrins and calix[3]pyrroles. Nevertheless, these macrocycles and related compounds have so far been synthesized using three main approaches: (1) boron(III)-templated synthesis, (2) direct intramolecular macrocyclization enabled by core-modification or organometallic catalysis, and (3) ring tightening to complement strain energy with aromatic stabilization. This section summarizes the pros and cons of these approaches for the synthesis of contracted porphyrins.

2.1 Boron-templated synthesis

Boron(III) atoms are suitable templates for the synthesis of subporphyrins and subphthalocyanines, and most of these macrocycles have been reported as boron(III) complexes. Given the absence of other template atoms in their reported synthesis, the atomic radius of boron is likely to fit well into the cavity of the tripyrrolic ring system compared with other metal ions such as Zn^{2+}, Cu^{2+}, and Ni^{2+}, which are frequently used as templates for porphyrin and phthalocyanine synthesis.[40–42] In the first synthesis of boron(III)-subphthalocyanine (**1**), Meller and Ossko

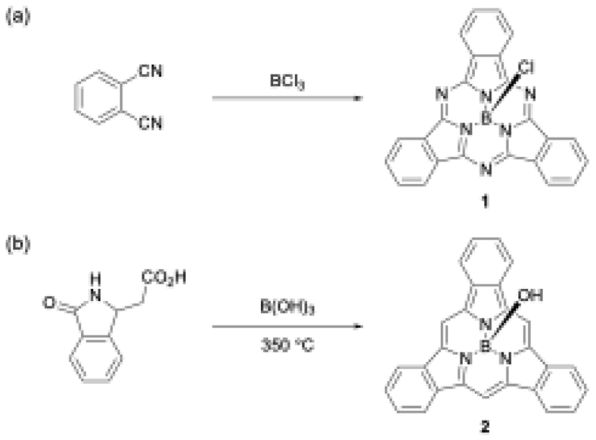

Scheme 1 First boron(III)-templated syntheses of (a) subphthalocyanine **1** and (b) tribenzosubporphyne **2**.

used haloboranes, such as BCl_3, both as a template and as an acid to activate phthalonitrile (Scheme 1).[30] Although the synthetic approach appeared to be applicable to subporphyrins, they have remained undiscoverable for more than 30 years. A possible reason for the failures in the subporphyrin synthesis is that haloboranes, which are strong Lewis's acids, promote hydrolytic B–N(pyrrole) bond cleavage in the presence of water and accelerate the polymerization of pyrrole monomers.

The first example of a subporphyrin, boron(III)–tribenzosubporphine (**2**), was synthesised in 2006 by combining Gouterman's tetrabenzoporphyrin synthesis[43] with a boron(III)-template. In this synthesis, boric acid was used as a template to promote the cyclotrimerization of an isoindole moiety generated from 2-(3-oxo-2,3-dihydro-1*H*-isoindol-1-yl)acetic acid at 350 °C (Scheme 1).[26] The boron center in **2** is initially coordinated by a hydroxo ligand, which is easily converted into the less-polar methoxo group by dissolving **2** in methanol for separation by silica gel column chromatography. Owing to the ineffective template effect of boric acid, **2** was isolated in only 1.4% yield.

Shortly after the first report of **1**, Kobayashi disclosed the synthesis of *meso*-aryl-substituted subporphyrins **4–6** using tri-*N*-pyrrolylborane (**3**)[44] as a precursor (Scheme 2). Although the B–N bonds in precursor **3** readily dissociate to release pyrrole in the presence of a strong Brønsted acid, Kobayashi's group used propionic acid as a mild acid for condensation with aldehyde under Adler's conditions to obtain **4** in approximately 5% yields after tedious chromatographic separation.[45]

When pyridine is coordinated to the boron center of **3**, the resulting pyridine-tri-*N*-pyrrolylborane (**7**)[46] can be used as a more soluble and slightly moisture- and acid-stable precursor for subporphyrin synthesis. Osuka and coworkers also successfully synthesized *meso*-aryl-substituted subporphyrins with various aryl groups, namely **8–10**, in 2–6% yields using **7** and trifluoroacetic acid (TFA) as a catalyst (Scheme 2).[47] Osuka's group isolated **8–10** in the B–OMe forms, which are quantitatively obtained from the B–OH forms upon heating in methanol and become less polar on silica gel. Aerobic oxidation in the synthesis of *meso*-aryl-subporphyrins often produces subchlorins, β,β-reduced subporphyrin analogues, as byproducts.[48]

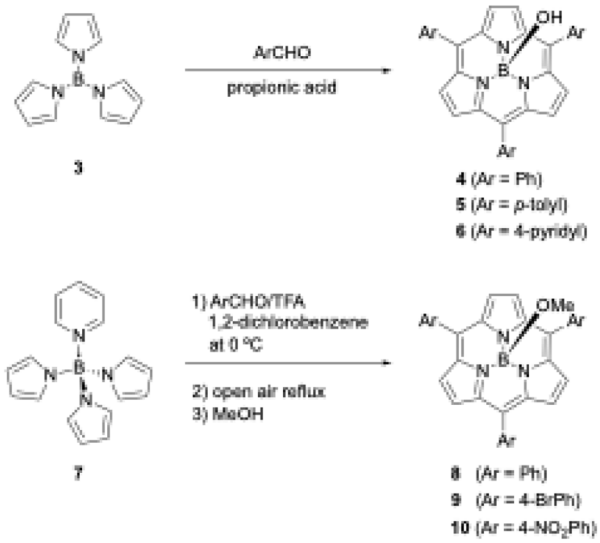

Scheme 2 Synthesis of *meso*-aryl-substituted subporphyrins using tri-*N*-pyrrolylborane derivatives as precursors.

Oxidation of subchlorins with MnO_2 improves the isolate yield of **8** from 3.8% to 6.3%. Although tri-*N*-pyrrolylborane derivatives allow the introduction of various *meso*-aryl substituents to the boron(III)-subporphyrin skeletons, synthetic yields remain below 10%, and considerable amounts of tetraarylporphyrin byproducts are always generated as a result of B–N bond cleavage.

Boron(III)-templated synthesis is more versatile and efficient with tripyrrane precursors than with tri-*N*-pyrrolylboranes. Triethylamine–boron(III)-tripyrromethene **12**,[49] which is generated *in situ* from tripyrromethene **11** and $BH_3 \cdot NEt_3$, gives subporphyrin **8** in 18% yield upon treatment with benzoyl chloride (Scheme 3).[50] Precursor **12** is also useful for the synthesis of A_2B-type and *meso*-free subporphyrins **13** and **14**, including subporphine **15**.[51] *Meso*-free subporphyrins provide good scaffolds for the construction of subporphyrin oligomers *via* bromination with *N*-bromosuccinimide and subsequent cross-coupling reaction using organometallic reagents.

Boron(III)-templated subporphyrin synthesis using *N*-pyrrolylborane precursors still has an unsolved question. Given the

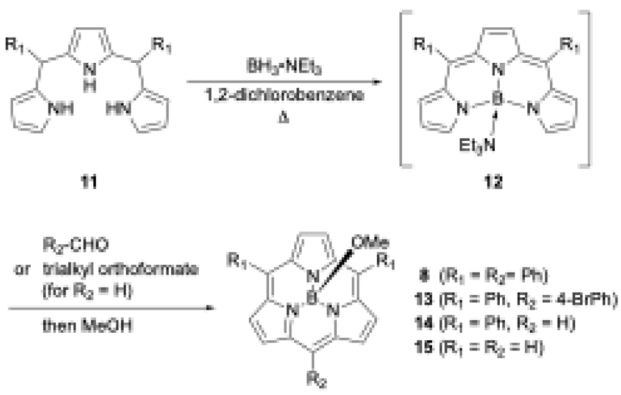

Scheme 3 Synthesis of A_2B-type subporphyrins including *meso*-free analogues.

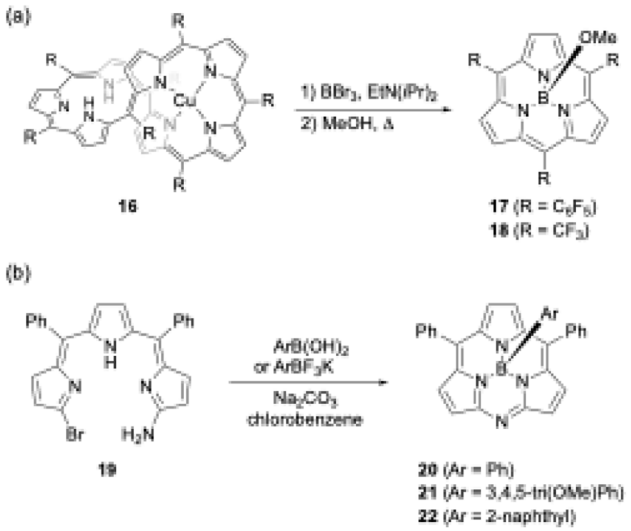

Scheme 4 (a) Metathesis-like ring splitting of heptaphyrin **16**, and (b) boron-templated synthesis of submonoazaporphyrins.

well-known reaction mechanism of porphyrin synthesis,[52] boron(III)-subporphyrinogen is considered the most likely intermediate of boron(III)-subporphyrins. However, no such intermediate has been observed during subporphyrin synthesis. Furthermore, the presence of intermediate **12** in the tripyrrane-based synthesis suggests the existence of an alternative reaction pathway leading to subporphyrins that does not involve subporphyrinogen-like intermediates. Understanding the detailed reaction mechanism of boron(III)-templated subporphyrin synthesis may hold the key to further improving the synthetic yields of subporphyrins.

Another unique boron(III)-templated subporphyrin synthesis is the metathesis-like ring splitting reaction of [32]heptaphyrin(1.1.1.1.1.1.1) Cu(II) complex **16** (Scheme 4a).[53,54] Upon boron(III) complexation, the heptapyrrolic macrocycle splits into boron(III)-subporphyrin and copper(II)-porphyrin. Although the scope of *meso*-substituents is limited, *meso*-pentafluorophenyl- and trifluoromethyl-substituted subporphyrins **17** and **18** are obtained from corresponding heptaphyrins in 36% and 6% yields, respectively.

Recently, a useful method for the high-yield synthesis of boron(III)-submonoazaporphyrins **20–22**, a hybrid-type macrocycle of subporphyrin and subporphyrazine,[55] was reported by Jiao and co-workers (Scheme 4b).[56] Jiao's group used α-amino-α′-bromotripyrromethene precursor **19** for the intramolecular nucleophilic substitution induced by boron(III)-complexation. Because arylboronic acid derivatives can be used as a template, various axial ligands are directly introduced onto the boron in high yields (≥70%), enabling facile perpendicular functionalization of the macrocycles.

2.2 Direct macrocyclization

Organometallic reagents and/or core-modifications have recently enabled the direct macrocyclization of tripyrrolic ring systems without boron templates. Interestingly, incorporation of an additional carbon atom at the *meso*-position of the triphyrin(1.1.1) skeleton enables acid-catalyzed condensation, which leads directly to triphyrin(2.1.1) macrocycles. Direct macrocyclization of triphyrins(2.1.1) and *meso*-expanded calix[3]pyrroles also enables the synthesis of various heteroarene-embedded analogues.

A recent striking finding in this research field is the Pd-catalyzed synthesis of subporphyrin free-bases by Osuka, Song, and coworkers.[31] The group coupled α,α′-diborylated tripyrrane precursor **23** to 9,10-bis(dibromomethylene)-substituted anthracene **24** in the presence of Sphos Pd G2 catalyst. Although the isolated yields were low (6%, 4%, and 2% for **25**, **26**, and **27** respectively), subporphyrin free-bases **25–27** were fully characterized using NMR and X-ray crystallographic analyses. The ^{1}H NMR spectrum of boron-free macrocycle **25** in $CDCl_3$ showed an up-field shift of the inner NH protons at 3.99 ppm, indicating that its 14π-aromatic nature is comparable with that of boron(III)-coordinated analogues. However, in the crystal structure of **14**, the tripyrrolic macrocycle adopts a non-planar, partial cone conformation (see Section 3.1) (Scheme 5).

Meso-expansion renders contracted porphyrin macrocycles more accessible through both acid-catalyzed condensation and organometallic means. Triphyrin(2.1.1) is a ring-contracted porphyrin bearing three pyrrole units and four *meso*-carbon atoms. The first examples of [14]triphyrins(2.1.1) **29–31** were serendipitously synthesized in approximately 35% yields by Yamada and coworkers through $BF_3\cdot OEt_2$-catalyzed Rothemund-type condensation of bicyclo[2.2.2]octadiene-fused pyrrole **28** and arylaldehyde (Scheme 6).[57] Following this first report, Yamada's group found that the amount of $BF_3\cdot OEt_2$ is critical for the selectivity of triphyrin(2.1.1) over expected porphyrin.[58] Although the detailed reaction mechanism is still unclear, the *meso*-vinylene bridge is formed by two formyl groups of the arylaldehyde. Bicyclo[2.2.2]octadiene-fused triphyrins(2.1.1) **29–31** were quantitatively converted into tribenzotriphyrins(2.1.1) **32–34** upon heating at 220 °C under reduced pressure, in a similar fashion as tetrabenzoporphyrin synthesis.[59]

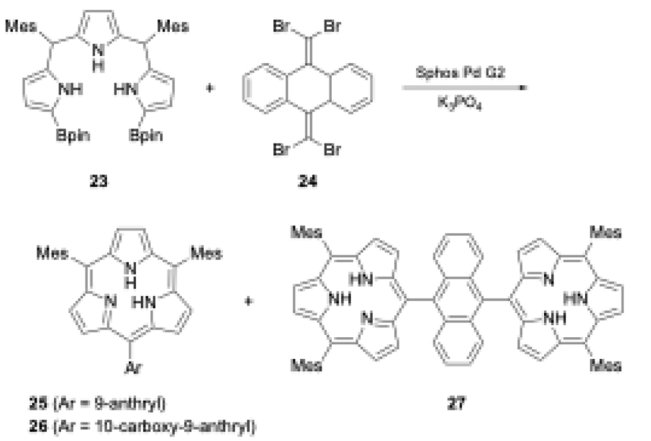

Scheme 5 Synthesis of subporphyrin free-bases through Pd-catalyzed cross-coupling reaction. (Bpin: pinacolatoboryl; Mes: mesityl).

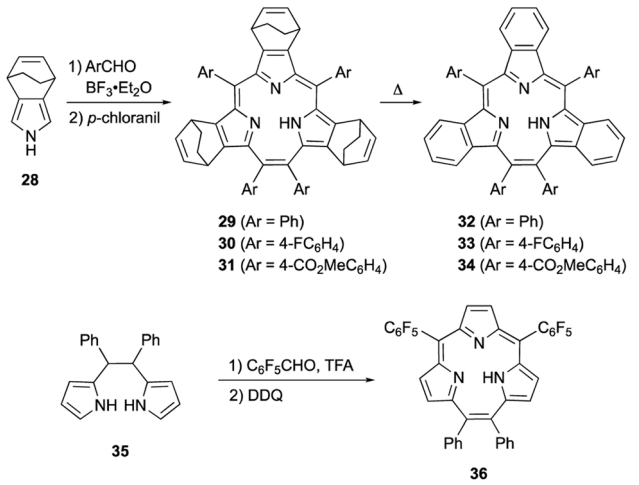

Scheme 6 Acid-catalyzed direct macrocyclization of triphyrin(2.1.1) analogues.

Rothemund-type protocols are also applicable to dipyrrolylethane precursor **35**. Condensation of **35** with pentafluorobenzaldehyde in the presence of TFA followed by DDQ oxidation furnished triphyrin **36** in 5% yield.[60] Without the addition of a pyrrole monomer to the reaction, the third pyrrole unit is likely generated through an acid-catalyzed scrambling process.[61]

Triphyrins(2.1.1) can also be synthesized through the McMurry coupling reaction. Intramolecular cyclization of α,α′-diformyltripyrrane precursor **37** using $TiCl_4$, Zn, and CuCl and subsequent oxidation of the resulting macrocycle gave triphyrin(2.1.1) **38** in 16% yield (Scheme 7).[62] Unlike acid-catalyzed synthesis, the McMurry coupling reaction enables the synthesis of *meso*-free triphyrins(2.1.1) in moderate yields.[62] When the McMurry coupling strategy is applied to dimethylmethylene-linked tripyrrane **39**, a *meso*-expanded calix[3]pyrrole analogue **40** is obtained in 33% yield through Pd/C catalyzed hydrogenation of the vinylene bridge.[63]

Core-modification enables the direct macrocyclization of triphyrin and calix[3]pyrrole analogs containing various

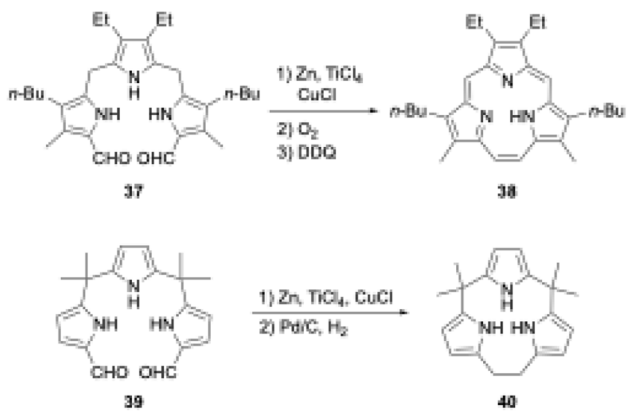

Scheme 7 McMurry coupling-based synthesis of triphyrin(2.1.1) and *meso*-expanded calix[3]pyrrole.

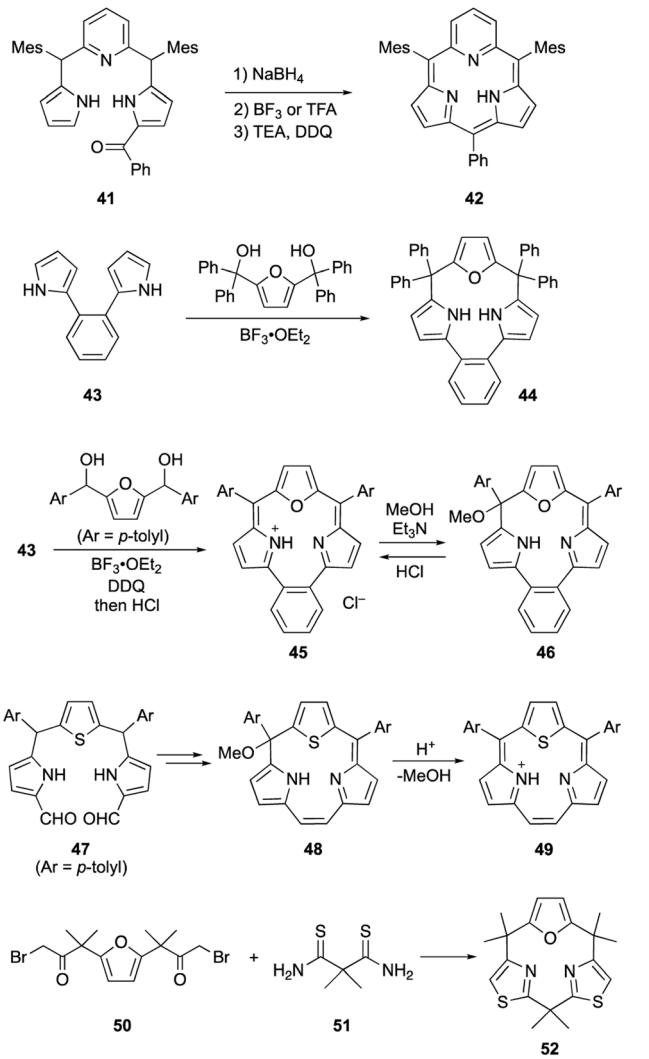

Scheme 8 Synthesis of various heteroarene-embedded triphyrin and calix[3]pyrrole analogues.

heteroarenes, such as furan and pyridine, instead of pyrrole units. Pyridine-embedded tripyrrane analogue **41** undergoes acid-catalyzed intramolecular cyclization in the carbinol form, which is generated *in situ* by reduction with $NaBH_4$. Following oxidation with DDQ, subpyriporphyrin **42** is obtained in 6% yield (Scheme 8).[64] Unlike subporphyrin free-bases, **42** exhibits non-aromatic characteristics, as indicated by its ^{1}H NMR spectrum, although **42** adopts a slightly ruffled yet planar conformation in the crystalline state. The key to this direct macrocyclization is the reduced number of NH protons and wide connection angles of the pyridine moiety.

Latos-Grażyński's group used 1,2-dipyrrolylbenzene **43** to synthesize furan-embedded calix-triphyrin **44** and oxatriphyrin **45**.[65] $BF_3 \cdot OEt_2$-catalyzed condensation of **43** with bis(hydroxydiphenylmethyl)furan affords **44** in 65% yield, while that with 2,5-bis(hydroxymethyltolyl)furan followed by DDQ oxidation and counterion exchange using HCl gives protonated **45** in 20% yield. Upon treatment with a 1 : 1 mixture of Et_3N/MeOH, oxatriphyrin **45** was quantitatively converts into phlorin-type macrocycle **46**.

The transformation between **45** and **46** is reversible because acidic removal of the methoxy group of **46** recovers **45**. A similar conversion also occurs with thiophene-embedded triphyrin(2.1.1) analogue **48**, which is obtained from tripyrrane **47** using the McMurry coupling reaction.[66] Stepwise addition of TFA to a dichloromethane solution of **48** increases the intensity of the Soret-like band at 414 nm in the UV-vis absorption spectrum of **49**, indicating the 14π-aromatic nature of **49**.

Recently, our group achieved direct macrocyclization of a calix[3]pyrrole analogue through strain-based molecular design for the feasible synthesis.[67] Although macrocyclic ring strain is considered as a key factor for the macrocyclization of contracted porphyrinoids, it is invisible and often unpredictable in complex ring systems. Our group applied the lowest energy conformation search using the artificial force induced reaction (AFIR)[68] to various heteroarene-replaced analogues of calix[3]pyrrole and, furthermore, visualized/evaluated their ring strain using the *StrainViz*[69] analysis developed by Jasti and coworkers. As a result, we found that calix[1]furan[2]thiazole (**52**) is less strained than the parent calix[3]pyrrole. In fact, a Hantzsch-type thiazole formation reaction between **50** and **51** proceeds under neutral conditions and desired **52** is obtained in 60% yield. This demonstrates the importance of pre-synthetic strain evaluation using theoretical calculations for feasible macrocyclization of contracted porphyrinoids.

2.3 Ring tightening approach

Aromatic rings are typically planar, and thus cyclooligomerization of aromatic subunits tends to produce linear oligomers and less-strained (larger) macrocycles rather than strained macrocycles. However, once precursor macrocycles are preorganized using conformationally flexible, non-aromatic synthons for aromatic subunits, the strain energy of the target macrocycles can be compensated for by the aromatic stabilization energy. Organic chemists have developed useful synthons to obtain elusive macrocycles with this ring tightening approach. As a representative example, [*n*]cycloparaphenylenes have been synthesized from precursor macrocycles composed of 1,4-diaryl-1,4-dialkoxycyclohexane or its cyclohexadiene analogues as *para*-phenylene synthons.[70–72]

In porphyrin-related chemistry, Kohnke and coworkers introduced a non-conventional method to synthesize calix[*n*]pyrroles and hybrid-type calix[*n*]furan[*m*]pyrroles using polyketone macrocycles.[73] Because 1,4-diketone unit can generate a pyrrole ring *via* the Paal–Knorr reaction, calix[*N*]pyrroles are successfully synthesized from cyclic *N*-mers of 3,3-dimethylpentane-2,4-dione (**53**).[74,75] In this calixpyrrole synthesis, the 5*N*-membered polyketone rings are contracted to 4*N*-membered rings. Although this approach was considered applicable to the synthesis of calix[3]pyrroles, promising hexaketone precursors, such as **59** in Scheme 9, were unavailable, because these polyketone precursors have been derived from calix[*n*]furans ($n \geq 4$), which are obtained through acid-catalyzed cyclooligomerization of furans.

To realize the ring tightening synthesis of calix[3]pyrrole, our group has developed stepwise oligomerization[76,77] and

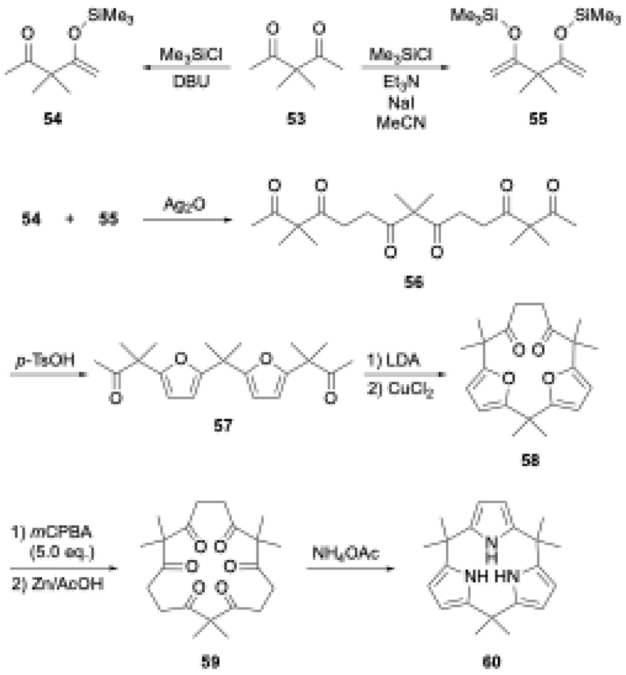

Scheme 9 First synthesis of calix[3]pyrrole.

macrocyclization[78] of acetylacetone derivative **53**. Compound **53** undergoes mono- and bis-selective silylation in the presence of 1,8-diazabicyclo[5.4.0]-7-undecene (DBU) and triethylamine to give **54** and **55**,[79] respectively. Linear trimer **56** is obtained in 27% yield by Ag_2O-mediated oxidative coupling between **54** and **55**. Although intramolecular cyclization of the terminally bis-silylated analogue of **56** with Ag_2O is unsuccessful, protection of the internal ketones by furan formation allows the use of lithium diisopropylamide (LDA)/$CuCl_2$. Intramolecular cyclization of **57** indeed proceeds to give difuran macrocycle **58** in 42% yield. The desired hexaketone precursor **59** is obtained in 28% yield through oxidative furan ring opening reaction of **58** using excess *m*-chloroperbenzoic acid (*m*CPBA) followed by Zn reduction.

Calix[3]pyrrole **60** was first synthesized in 41% yield through a triple Paal–Knorr reaction using cyclic hexaketone **59** and ammonium acetate (Scheme 9). An important factor in the successful synthesis of **60** is the use of non-acidic reaction conditions because acids commonly used under Rothemund–Lindsey conditions, such as TFA, trigger rapid, quantitative strain-induced ring expansion of **60**, which will be discussed in Section 3.

The ring tightening approach using cyclic oligoketone precursors also enables the synthesis of furan- and thiophene-embedded calix[3]pyrrole analogues (Scheme 10). Dehydrative furan ring formation reaction of **58** using chlorotrimethylsilane and P_2O_5 in methanol furnishes calix[3]furan (**61**) in 53% yield,[80] which is inaccessible *via* acid-catalyzed condensation. Pyrrole ring formation reaction of **58** gives calix[2]furan[1]pyrrole (**62**) in 79% yield. The addition of 3 equivalents of *m*CPBA to **58** affords monofuran macrocycle **63** in 71% yield after reductive workup using Zn. Macrocycle **63** is further

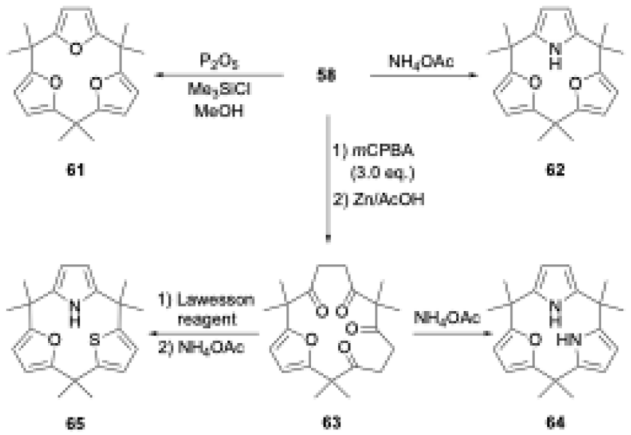

Scheme 10 Ring tightening synthesis of calix[3]pyrrole analogues.

converted into calix[1]furan[2]pyrrole (**64**) and calix[1]furan[1]pyrrole[1]thiophene (**65**) using ammonium acetate and Lawesson's reagent.[81] The synthesis of calix[3]pyrrole analogues based on cyclic polyketones has provided insight into their ring strain-induced chemical properties.

3. Ring-contraction effects

Until ring-contracted porphyrins and calixpyrroles were first synthesized, they were mainly recognized as synthetic targets rather than functional molecules. Recent studies on their structural, optical, chemical, and supramolecular properties, however, have gradually revealed the effects of ring-contraction on their porphyrin-like yet tripyrrole-unique macrocycles. This section summarizes the unique properties of contracted porphyrinoids, which are not commonly observed in other porphyrins or expanded porphyrins.

3.1 Macrocyclic structures

Boron(III)-subporphyrins typically have a bowl-shaped structure owing to the tetrahedral coordination geometry of the boron center. The subporphyrin macrocycle behaves as a dianionic tridentate ligand, and the boron center has an anionic axial ligand that is coordinated perpendicular to the macrocycle, forming a neutral complex. Boron(III)-subporphyrins can adopt a planar conformation with a tricoordinated boron center upon the generation of borenium cation species.[82] Borenium cation with an inert carborane counterion has been crystallographically analyzed by Reed's group. Although a similar subphthalocyanine borenium cation[83] adopts a bowl-shaped conformation (bowl-depth of 1.073 Å), subporphyrin **66** is almost planar with a bowl-depth of 0.114 Å (Fig. 2, see also Scheme 11 in Section 3.3). NMR and X-ray crystallographic analyses indicated that boron(III)-subporphyrins interconvert between planar borenium and bowl-shaped neutral forms in acidic solutions.

The remarkable ring-contraction effects also occur in *meso*-aryl-substituted boron(III)-subporphyrins. Although *meso*-tetraphenylporphyrin has four phenyl groups arranged almost

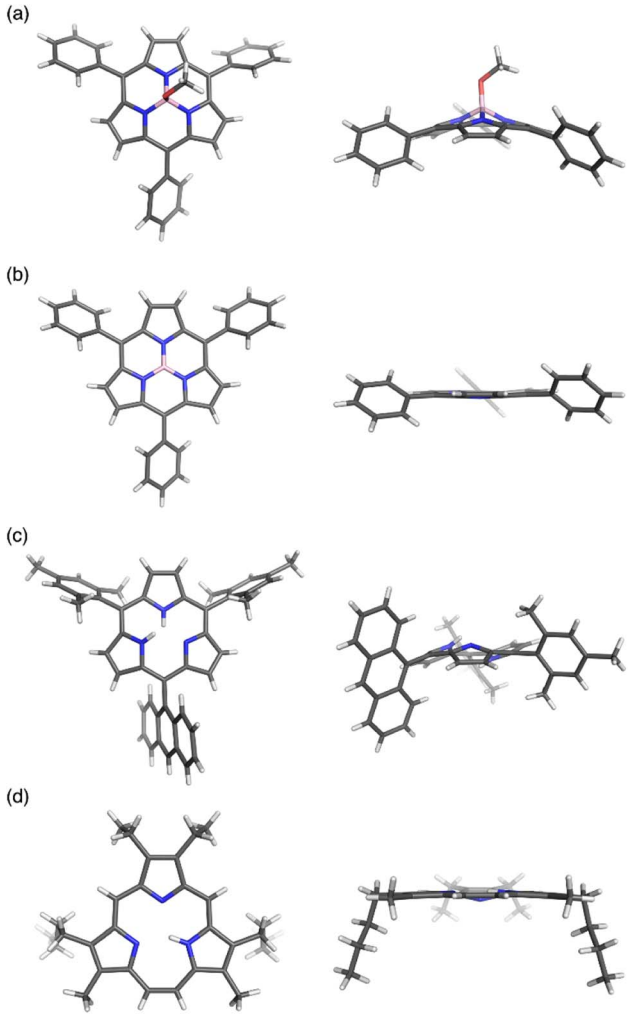

Fig. 2 X-ray crystal structures of (a) *meso*-phenyl subporphyrin **8**, (b) subporphyrin borenium cation **66**, (c) subporphyrin free-base **25**, and (d) triphyrin(2.1.1) **38**. Left: top view, right: side view.

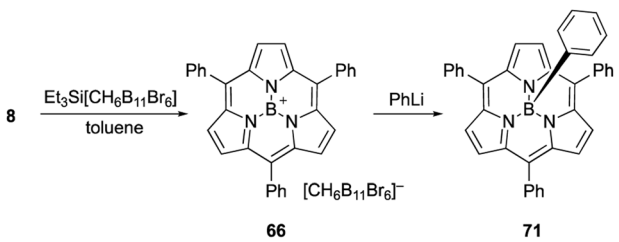

Scheme 11 Formation of subporphyrin–borenium cation species for subsequent introduction of axial phenyl ligand.

perpendicular to the porphyrin ring, subporphyrin **8** has phenyl groups tilted at 38 to 48° in the crystalline state.[47] This suggests that the *meso*-aryl groups of subporphyrins experience a decreased rotational barrier and thus increased substituent effects through π-conjugation (discussed in the Section 3.2).

Boron-free subporphyrin **25** adopts a non-planar, partial cone-like conformation, despite its fully conjugated 14π-aromatic nature.[31] This can be attributed to the repulsive

interactions between the two NH groups inside the narrow cavity. In contrast, planar conformations are adopted by triphyin(2.1.1) free-bases such as **38**. Triphyrins(2.1.1) have an NH and two iminic nitrogen atoms in cavities that are slightly larger than those of subporphyrins. Therefore, the NH protons preferentially form hydrogen bonds with iminic nitrogen atoms on the same plane.

Calix[3]pyrrole **60** exhibits an unusually strained macrocyclic structure in the crystalline state. In its monohydrated form, **60** adopts a partial cone conformation, with one pyrrole unit oriented toward the opposite side of the other units (Fig. 3). Notably, the *meso*-carbon atoms are out of the mean plane of the neighboring pyrrole rings, suggesting a highly strained structure of **60**. Their deformation angles α and β,[84] which are used to evaluate the displacement around the aromatic rings embedded in a macrocycle, are 2.52° and 9.20°, respectively.[32] These values are remarkably larger than those of calix[4]pyrrole ($\alpha = 0.38°$, $\beta = 1.60°$). Theoretical calculations revealed that calix[3]pyrrole **60** is 22.1 kJ mol^{-1} more unstable per repeat unit than calix[4]pyrrole **67**.

Pyrrole/furan hybrid type calix[3]pyrrole analogues, calix[2]furan[1]pyrrole **62** and calix[1]furan[2]pyrrole **64**, adopt cone and partial cone conformations, respectively. The deformation angles of the pyrrole units, α and β, are respectively 2.48° and 6.17° in **62** and 2.49° and 8.52° in **64**. These observations indicate that the displacement of the pyrrole units diminishes as the number of pyrrole units decreases. Calix[3]furan **61** adopts a cone conformation in the crystalline state, and its deformation angles around the furan rings are smaller than those in calix[2]furan[1]pyrrole **62**.[80]

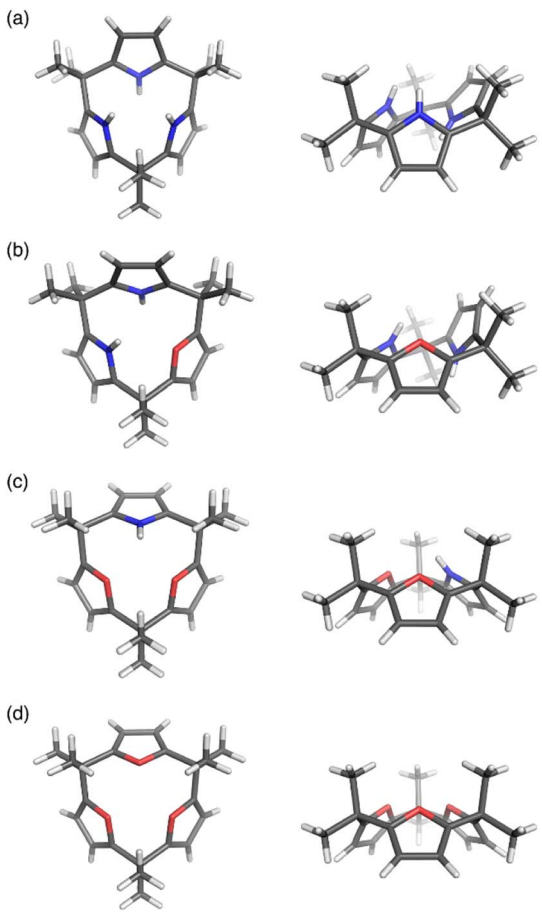

Fig. 3 X-ray crystal structures of (a) calix[3]pyrrole **60**, (b) calix[1]furan[2]pyrrole **64**, (c) calix[2]furan[1]pyrrole **62**, and (d) calix[3]furan **61**. Left: top view, right: side view.

3.2 Optical and electrochemical properties

Subporphyrins are characterized by 14π-conjugated aromatic macrocycles that exhibit larger HOMO–LUMO gaps and blue-shifted absorption/emission bands compared with the corresponding porphyrins comprising 18π-aromatic macrocycles. *Meso*-triphenylsubporphyrin **8** displays a Soret-like band at 373 nm and Q-like bands at 450–500 nm in CH_2Cl_2 (Fig. 4). In contrast to the Zn(II) complex of *meso*-tetraphenylporphyrin (**Zn-TPP**),[85] which is red in solution, **8** is yellowish orange and emits green fluorescence with a fluorescence quantum yield of 13%. The first oxidation and reduction potentials of **8** are observed at 0.78 and −1.82 eV *versus* the ferrocene/ferrocenium (Fc/Fc^+) couple,[47] while those of **Zn-TPP** lie at 0.76 and −1.41 eV, respectively.[86] The larger electrochemical HOMO–LUMO gap of **8** (2.60 eV) in comparison to **Zn-TPP** (2.17 eV) is consistent with the bule-shifted Q-like bands observed in the absorption spectrum of **8**.

The optical properties of subporphyrins can be widely modulated by the substituent effects of *meso*-aryl groups. Substitution of the *N*,*N*-dialkylamino group at the *p*-position of the *meso*-phenyl group leads to a remarkable red-shift of the absorption and emission bands of **68** with an increased fluorescence quantum yields up to 60%.[87] This is attributed to intramolecular charge transfer interactions between the

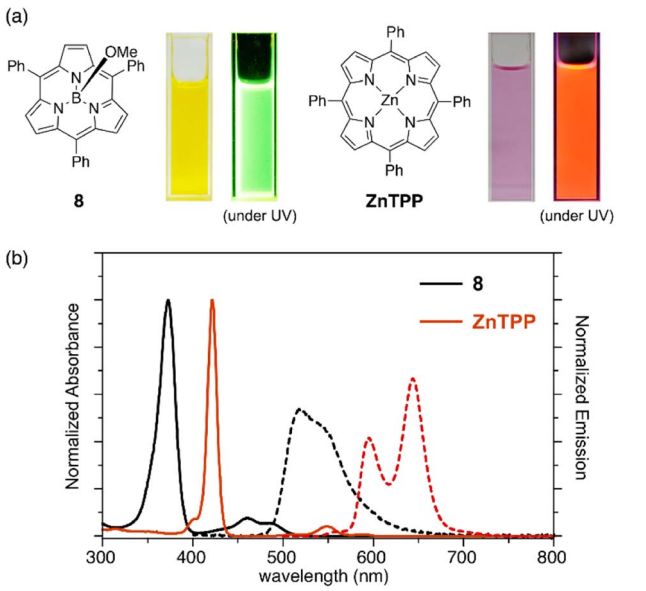

Fig. 4 (a) Photographs of CH_2Cl_2 solutions of **8** and ZnTPP under room light and UV light. (b) UV-vis absorption (solid line) and emission (dashed line) spectra of subporphyrin **8** and tetraphenylporphyrin (ZnTPP) in CH_2Cl_2.

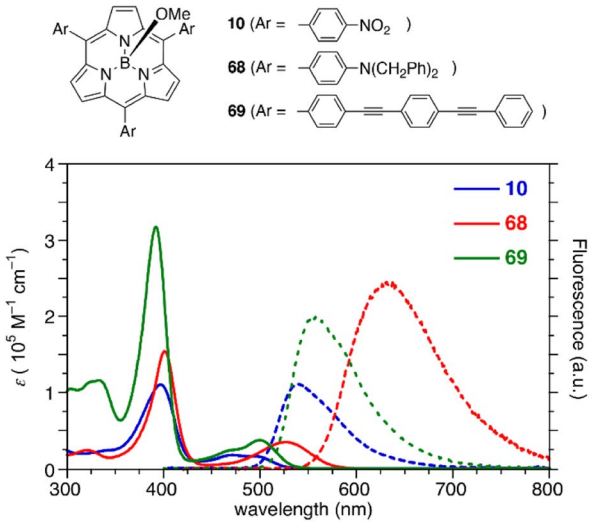

Fig. 5 UV-vis absorption (solid line) and fluorescence (dashed line) spectra of subporphyrins **10**, **68**, and **69** bearing 4-substituted phenyl groups at the *meso*-positions in CH_2Cl_2.

electron-donating amino group and the low-lying LUMO of the subporphyrin core. The substituent effects at the *p*-position of the *meso*-phenyl group are typically trivial in tetraphenylporphyrins because of the high rotation barrier and almost perpendicular orientation of the *meso*-phenyl groups.[88] In contrast, the optical properties of *meso*-aryl subporphyrins are significantly perturbed by the substituents. For example, 4-nitrophenyl-substituted subporphyrin **10** (ref. 47) shows solvent-dependent absorption and fluorescence. Moreover, π-conjugation of the *meso*-substituents on oligo(1,4-phenyleneethynylene)[89] substituted analogue **69** significantly increases the absorption coefficient of the Soret-like band (Fig. 5).

Ring contraction also affects the optical properties of calix[3]pyrrole analogues whose π-conjugation is interrupted at the *meso*-sp^3-carbon atoms.[90] Although calix[4]pyrrole (**67**) and calix[6]pyrrole (**70**) give rise to nearly identical absorption spectra derived from the π–π* transition of the pyrrole units, calix[3]pyrrole **60** exhibits a broad red-shifted band at 265 nm. Non-covalent interaction (NCI) plot analysis indicates that the

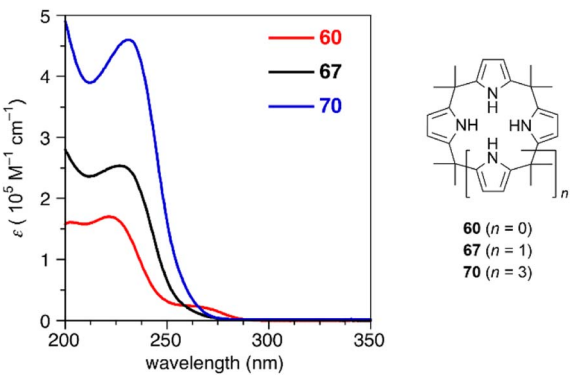

Fig. 6 UV-vis absorption spectra of calix[*n*]pyrroles (n = 3, 4, 6) in acetonitrile.

contracted ring system enhances through-space interactions between neighboring pyrrole rings. Similar intramolecular interactions between the furan and pyrrole units in furan/pyrrole hybrid macrocycles **62** and **64** result in solvent-dependent Stokes shifts, indicating polar excited states. Such optical properties can be used as a probe to distinguish calix[3]-type macrocycles from other larger analogues (Fig. 6).

3.3 Strong boron chelation

Most subporphyrin and triphyrin analogues stably chelate a boron(III) atom in their cavity. Although various harsh conditions, such as heating with strong Lewis/Brønsted acids or treatment with organolithium reagents, have been applied to boron(III)-subporphyrins, removal of the boron atom to give free-base macrocycles has not yet been achieved. However, axial ligands on the boron center readily exchange with hydrogen, oxygen, carbon, and halogen-based monoanionic ligands. Therefore, the boron center in subporphyrins can serve as a rigid scaffold for the orthogonal functionalization of macrocycles.

The reaction of boron(III)-subporphyrin **8** with $Et_3Si[CH_6B_{11}Br_6]$, a silylium reagent, generates tri-coordinated borenium cation **66** without deboronation of the subporphyrin ligand (Scheme 11).[82] Treatment of **66** with phenyl lithium results in the formation of axially phenyl-substituted **71**.

The B–OH and B–OMe forms undergo various axial ligand exchange reactions (Scheme 12). Fluoro- and trifluoroacetoxo-substituted forms **72** and **73** are obtained through the reactions of **4** with $BF_3 \cdot OEt_2$ and TFA, respectively. These analogues can also be converted back into B–OH form **4** through hydrolysis. Upon heating in the presence of excess alcohol, the hydroxo group in **4** can also be replaced with an alkoxo ligand.[91] Methoxo form **8** can react with Grignard reagents, including aryl, alkynyl, and alkyl magnesium bromides, to form an axial B–C bond. For example, treatment of **8** with 20 equivalents of 1-naphthyl magnesium bromide results in the formation of **75** in 91% yield.[92] Upon treatment with diisobutylaluminium hydride (DIBAL-H), compound **8** affords subporphyrinato boron(III) hydride **74**, which is capable of hydroborating aldehydes and ketimines.[93] Borohydride **74** releases the hydride ion upon the addition of a tritylium cation, $Ph_3C[B(C_6F_5)_4]$, to give borenium cation species. Air oxidation of **74** slowly proceeds even in the solid state to give a boron peroxide **76**, which is also prepared from **8** by treatment with hydrogen peroxide. Interestingly, thermolysis of peroxide **76** in 1,2-dichlorobenzene results in the formation of peroxo-bridged dimer **77**. Analogous μ-oxo dimer **78** can be prepared from B–OH form **4** through the reaction with Et_3N.[94] Reversible and almost quantitative axial ligand exchange reactions have also been used to form molecular assemblies of subporphyrins (see Section 3.6).

Triphyrin(2.1.1) and calix[3]pyrrole can also form acid-stable boron(III) complexes. Treatment of triphyrin(2.1.1) **38** with $BPhCl_2$ leads to the formation of tetracoordinated boronium cation complex **79** (Scheme 13). Complexation with a boron(III) atom changes the conformation of the macrocycle from planar to bowl-shaped. Boron complexes of triphyrin(2.1.1) are stable to strong acids including concentrated HCl, HPF_6, and HBF_4

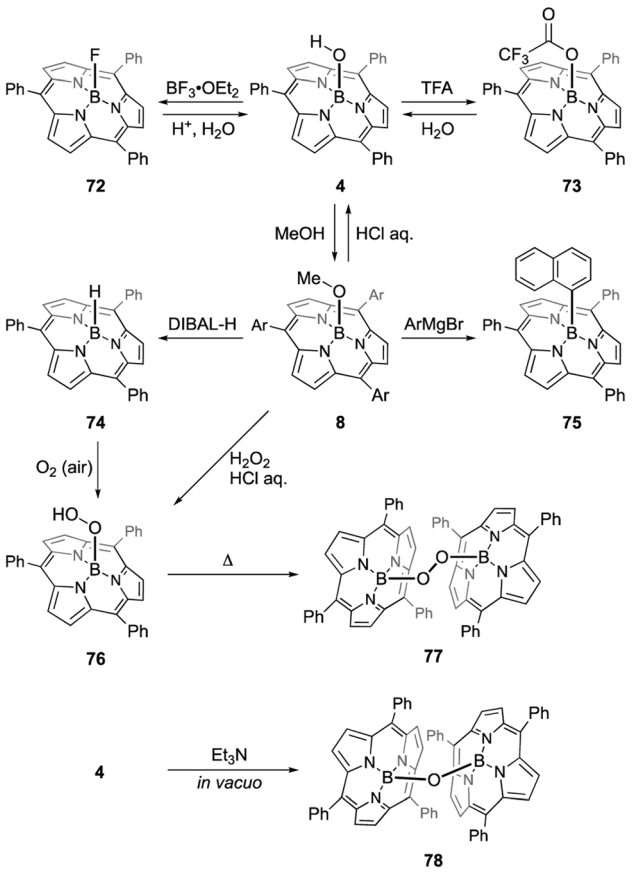

Scheme 12 Axial ligand exchange reactions of boron(III)-subporphyrins.

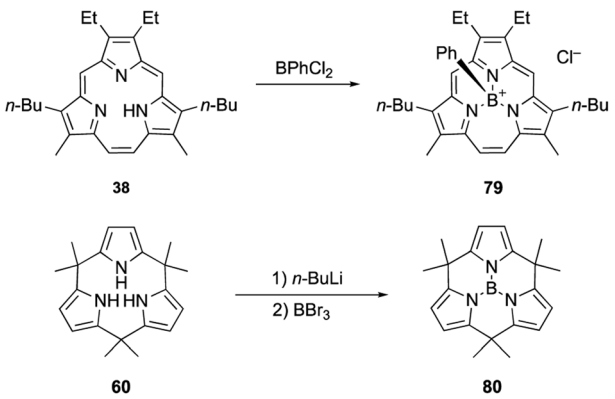

Scheme 13 Formation of acid-stable boron(III) complexes.

without deboronation.[95] Calix[3]pyrrole **60** also forms stable boron(III) complex **80** with a tricoordinated planar boron center. Although tri-*N*-pyrrolylborane **3** is susceptible to hydrolysis and acidolysis, resulting in the release of pyrrole monomers, boron complex **80** resists deboronation even after treatment with TFA.[32]

3.4 Metal complexation

Although the metal coordination of subporphyrin free-bases with boron(III) only has been reported so far, metal complexes of triphyrins(2.1.1) have been extensively studied. Because triphyrins(2.1.1) act as monoanionic tridentate ligands, they can form complexes with low-valent metal ions.

Complexation of *meso*-free triphyrin(2.1.1) **38** with $Mn(CO)_5Br$ and $Re(CO)_5Cl$ salts, furnish isostructural Mn(I) and Re(I) tricarbonyl complexes **81** and **82**, respectively.[62] The Mn(I) ion in **81** is coordinated by the three CO ligands and three nitrogen atoms of the triphyrin, resulting in an octahedral coordination geometry (Fig. 7). Triphyrin macrocycles **81** and **82** no longer maintained a planar conformation but adopt a slightly bowl-shaped structure, and the metal ion is not fully incorporated into the cavity. The first oxidation potentials of **81** and **82** are observed at 0.25 and 0.48 eV, respectively, *versus* Fc/Fc^+ couple. The shifted oxidation potentials of these complexes in comparison to that of the free-base analogue **38** (0.63 eV) indicate that the initial oxidation events occur at the metal centers.[62] Complexation of tribenzotriphyrin **34** with $[\{Fe(CO)_2(Cp)\}_2]$ (Cp: cyclopentadienyl) leads to the formation of sandwich complex **83** bearing a CpFe(II) unit and a bowl-shaped triphyrin ligand. The oxidation potential of the iron complex **83** is lower than that of ferrocene.[96]

Triphyrin(2.1.1) can also behave as a neutral bidentate ligand. Complexation with $PtCl_2$ and $PdCl_2$ salts results in the formation of complexes **84** and **85**, respectively.[97] These complexes exhibit a similar coordination, with the triphyrin(2.1.1) macrocycles adopting partial cone-like conformations and an uncoordinated NH site. The square-planar

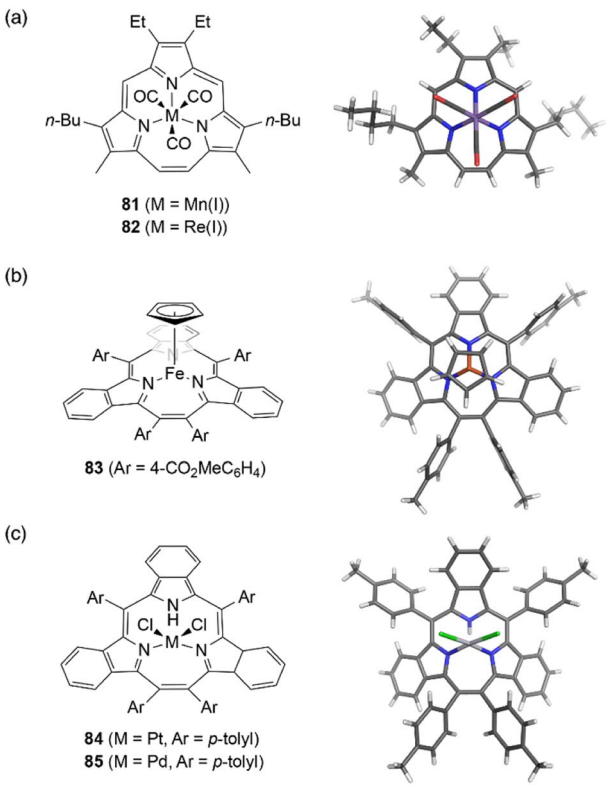

Fig. 7 Transition metal complexes of triphyrin(2.1.1). X-ray crystal structures of (a) Mn(I) complex **81**, (b) Fe(II) complex **83**, and (c) Pt(II) complex **84**.

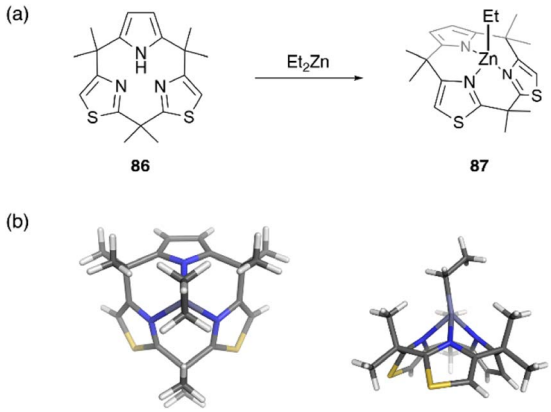

Fig. 8 Formation of moisture-stable organozinc complex **87** from calix[3]pyrrole analogue **86**. (a) Synthetic scheme and (b) crystal structure of **87**.

metal center is coordinated to two iminic nitrogen atoms and two chloride anions. Upon oxidation with molecular oxygen, Pt(II) complex **84** converts into a Pt(IV) complex with a bowl-shaped triphyrin conformation.[98] This indicates conformational flexibility of the triphyrin(2.1.1) macrocycles despite their 14π-aromatic nature.

Recently, metal complexes of a calix[3]pyrrole analogue, calix[1]pyrrole[2]thiazole **86**, have been reported,[67] with the ring contraction effect stabilizing the chelation of the ethyl zinc moiety. When **86** is treated with diethylzinc in toluene, ethylzinc complex **87** is obtained in 72% yield. X-ray crystallographic analysis reveals the cone conformation of calix[3]-related ligand **86**, which behaves as a monoanionic tridentate ligand. Because the ethylzinc moiety is sterically protected by the macrocyclic ligand, hydrolysis and alcoholysis of **87** are effectively suppressed even in the presence of excess water and alcohol in solution. In contrast, organozinc **87** is used as a catalyst for the polymerization of *rac*-lactide in refluxing toluene in the presence of benzyl alcohol (Fig. 8).

3.5 Strain-induced ring expansion

The macrocyclic ring strain of calix[3]pyrrole analogues induces unusual ring expansion reactions. Under Rothemund–Lindsey type acidic conditions, calix[3]pyrrole **60** quantitatively converts into calix[6]pyrrole **70** within 30 s (Scheme 14).[32] Calix[1]furan[2]pyrrole **64** exhibits similar reactivity to give calix[2]furan[4]pyrrole **88** in 95% yield after 5 min under the Rothemund–Lindsey conditions. In contrast, calix[3]furan **61** and calix[2]furan[1]pyrrole **62** do not undergo such ring expansion owing to their decreased ring strain. Upon *N*-methylation of the pyrrole moiety, however, methylated form **89** undergoes acid-catalyzed ring expansion, resulting in the formation of calix[6]-type products **91** and **92** in 32 and 18% yields, respectively.[80]

A detailed study of the reaction mechanism reveals that protonation of the pyrrole-α carbon initiates an irreversible and regioselective ring cleavage of calix[3]pyrrole analogues to give linear tripyrrane-like intermediates, such as **90**. The linear intermediates undergo cyclodimerization in a head-to-tail manner, resulting in the formation of calix[6]pyrrole-type

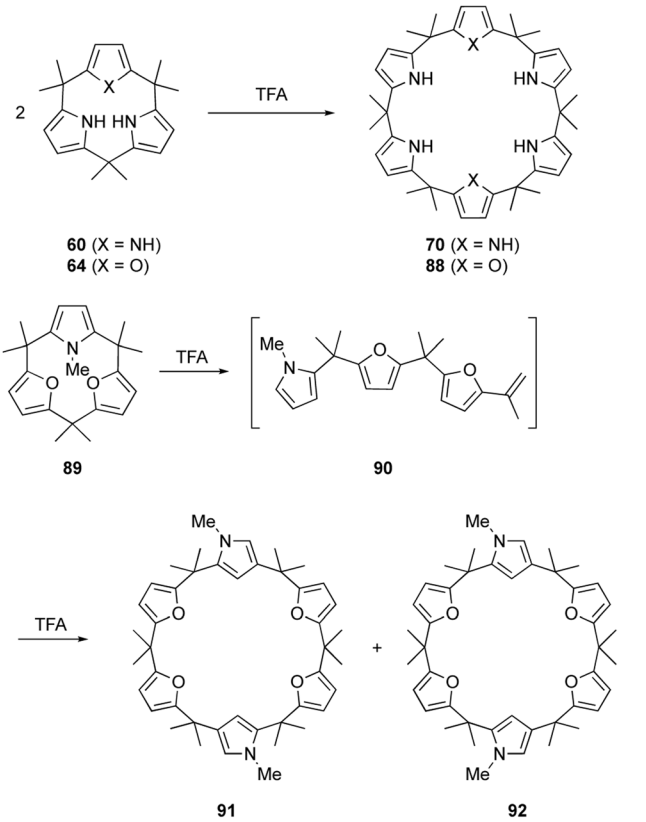

Scheme 14 Strain-induced ring expansion of calix[3]pyrrole analogues.

products. Rapid ring cleavage explains why calix[3]pyrrole-type macrocycles, including subporphyrinogens, have been missing during porphyrin or calix[4]pyrrole synthesis under Rothemund–Lindsey conditions.

Strain-induced ring expansion can be appled to obtain giant macrocycles, which are larger than the calix[6]pyrrole system. TFA-catalyzed strain-induced ring expansion of calix[1]furan[1]pyrrole[1]thiophene **65** produces calix[9]- and calix[12]-type macrocycles **94** and **95** in 16% and 7% yields, respectively, as well as calix[6]-type product **93** in 30% yield.[81] Single crystal X-ray diffraction analysis of **95** reveals its windmill-like conformation and perfect sequence selectivity (Fig. 9).

3.6 Supramolecular chemistry

The concave surface of bowl-shaped π-conjugated molecules is advantageous for molecular recognition of fullerenes. Boron(III)-subporphyrins can serve as good scaffolds for capturing fullerenes as well as corannulenes[99] and subphthalocyanines[100] through π–π interactions. Osuka and coworkers found that tris(1,4-benzodithiino)subporphyrin **96** binds fullerene C_{60} in solution and in the solid state. Job's and Foster–Fyfe plot analyses of NMR titration results reveal a 1 : 1 complexation of **96** and C_{60} in toluene-d_8 with an association constant of K_a of 857 ± 58 M^{-1} at 25 °C. Single crystal X-ray diffraction analysis reveals that all 1,2-benzenedithio groups are located on the concave side of **96**, enhancing π–π interactions with C_{60}

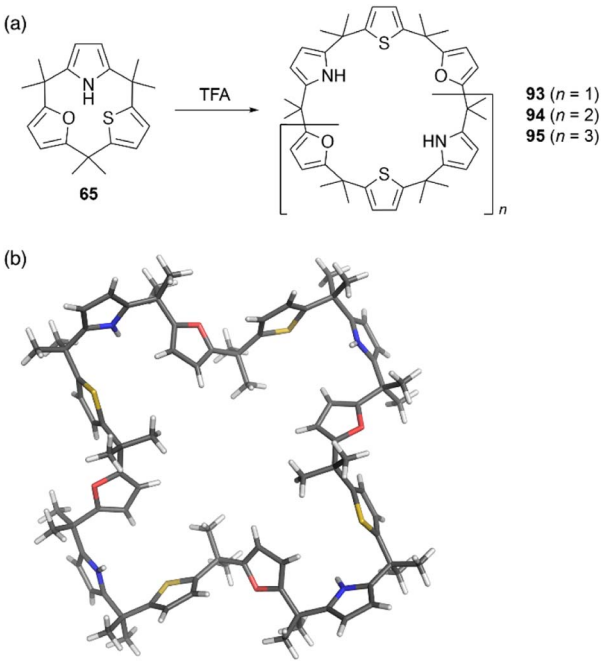

Fig. 9 (a) Strain-induced ring expansion of **65** and (b) X-ray crystal structure of calix[12]-type macrocycle **95**.

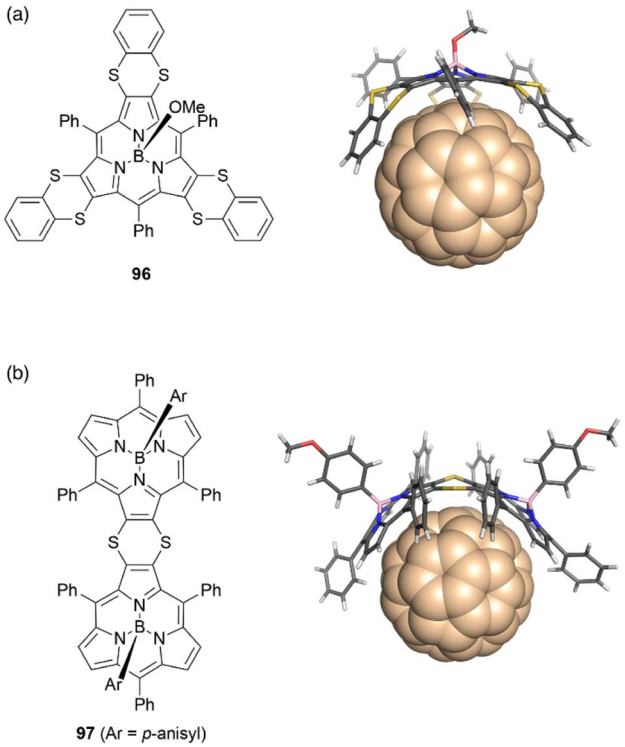

Fig. 10 Crystal structures of fullerene complexes (a) **96**·C_{60} and (b) **97**·C_{60}.

(Fig. 10).[101] Furthermore, *syn*-type β,β-(1,4-dithiino)subporphyrin dimer **97** and C_{60} engage in 1 : 1 binding in toluene, with a remarkably large association constant K_a of $(1.9 \pm 0.2) \times 10^6$ M^{-1}. In contrast, binding of **97** to C_{70} occurs with 2 : 1 stoichiometry characterized by association constants K_1 and K_2 of $(1.6 \pm 0.5) \times 10^6$ and $(1.8 \pm 0.9) \times 10^5$ M^{-1}, respectively.[102]

Axial ligand exchange at the boron(III) center helps to construct supramolecular assemblies of subporphyrins. Because alcohols and carboxylic acids can reversibly replace boron axial ligands, B–O bond formation on boron(III)-subporphyrins can be harnessed for dynamic covalent chemistry. Subporphyrin **98**, bearing a 2-carboxyphenyl group, quantitatively forms self-assembled dimer **99** through azeotropic removal of methanol in refluxing toluene (Scheme 15).[103] Dimerization of **98** is completed within 3 h at the concentration of 100 μM. Although dimer **99** is resistant to hydrolysis, heating in a mixture of dichloromethane/methanol results in the quantitative recovery of monomer **98**.

When *meso*-chloro-substituted subporphyrin **100** was treated with potassium hydroxide in DMSO, cyclic trimer **101** is obtained in 94% yield after aqueous workup (Scheme 15).[104] The chlorine atom at the *meso*-position is replaced with a hydroxy group as a result of the S_NAr reaction, and the subsequent axial ligand exchange with the *meso*-hydroxy group yields **101**. Although various cyclic oligomers are derived from *meso*-hydroxy subporphyrin, trimer **101** is obtained with remarkable selectivity. Trimer **101** dissociates into monomers upon treatment with TFA, potassium *t*-butoxide, or methanol.

Ring contraction also affects the anion binding properties of calix[*n*]pyrroles. Calix[4]pyrrole **67** is a well-known host for anion binding, with an association constant of $K_a = 17\,170 \pm$

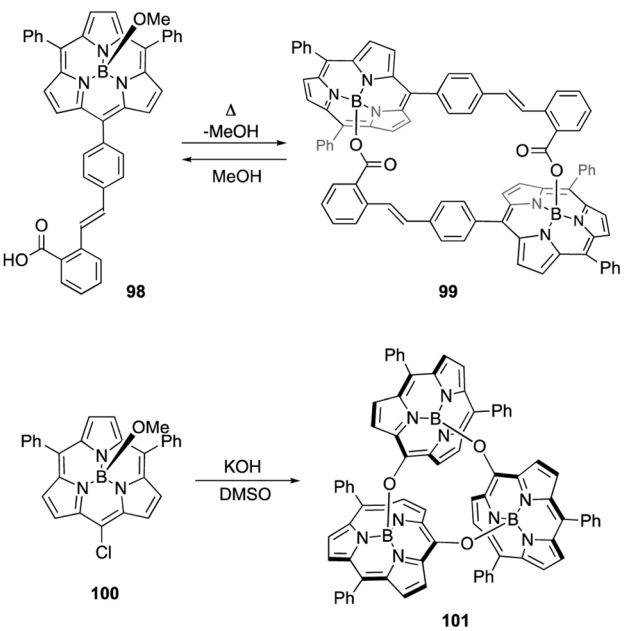

Scheme 15 Formation of molecular assemblies through boron axial ligand exchange.

900 M^{-1} in CD_2Cl_2 for fluoride binding. Upon anion binding, the solid state conformation of **67** changes from 1,3-alternate to cone (Fig. 11).[105] In contrast, binding of ring-contracted analogue, calix[3]pyrrole **60**, to the fluoride anion is characterized by a markedly small association constant (230 ± 20 M^{-1}).

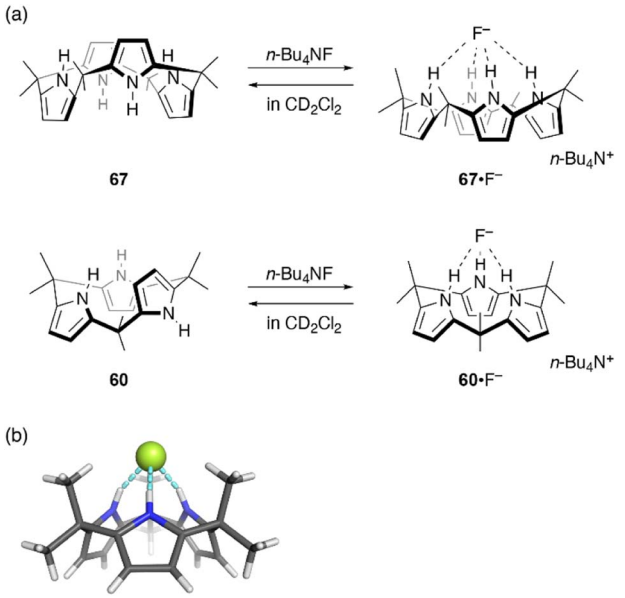

Fig. 11 (a) Fluoride binding to calix[4]pyrrole **67** and calix[3]pyrrole **60**. (b) Crystal structure of **60**·F⁻.

X-ray diffraction analysis of single crystals of **60**·F⁻, obtained as a tetrabutylammonium salt, reveals a cone conformation of **60** in which three NH sites are hydrogen bonded to the fluoride anion.[32] In addition to the reduced number of NH sites, the unstable cone conformation likely contributes to the reduced binding constant. Indeed, molecular dynamics (MD) simulations show the rapid and continuous flipping of pyrrole units in **60**, which interconverts between partial cone conformations.[106] The cone conformation is found to be energetically unfavorable in the absence of an anion.

Restricted flipping of calix[3]pyrroles allows the generation of inherently chiral macrocycles. The inherent chirality is the concept introduced by Böhmer in 1994 for asymmetrically substituted calix[4]arenes.[107] Although macrocycles have no stereogenic center, they display chirality because they belong to the C_1 point group. In the case of calix[4]pyrroles, rapid ring flipping render asymmetrically substituted analogues virtually achiral. MD calculations indicated that the ring flipping of calix[3]pyrrole analogue **65** is sufficiently slow for enantiomeric separation. Chiral resolution of **65** using an amylose-based chiral HPLC column leads to the separation of enantiomers, although their racemization through ring flipping in hexane/*i*-PrOH (v/v = 1 : 1) occurs with a half-life of 2.1 h.[81] When **65** is *N*-methylated using MeI/NaH, resulting **102** does not undergo racemization at room temperature even after standing for a month. The absolute configuration of each enantiomer is unambiguously determined through X-ray diffraction analysis. Enantiomerically pure forms, (R_p,S_p,S_p)-**102** and (S_p,P_p,P_p)-**102**, give rise to mirror-image circular dichroism (CD) spectra (Fig. 12). Furthermore, enantioselective *N*-methylation of **65** occurs in the presence of a chiral ammonium salt, (*R*)-4,4-dibutyl-2,6-bis(3,4,5-trifluorophenyl)-4,5-dihydro-3*H*-dinaphtho[2,1-*c*:1′,2′-*e*]azepinium bromide,[108] although enantioselectivity is modest (48% yield, 10% ee). This result demonstrates the potential of inherently chiral calix[3]pyrrole analogues for chiral molecular recognition.

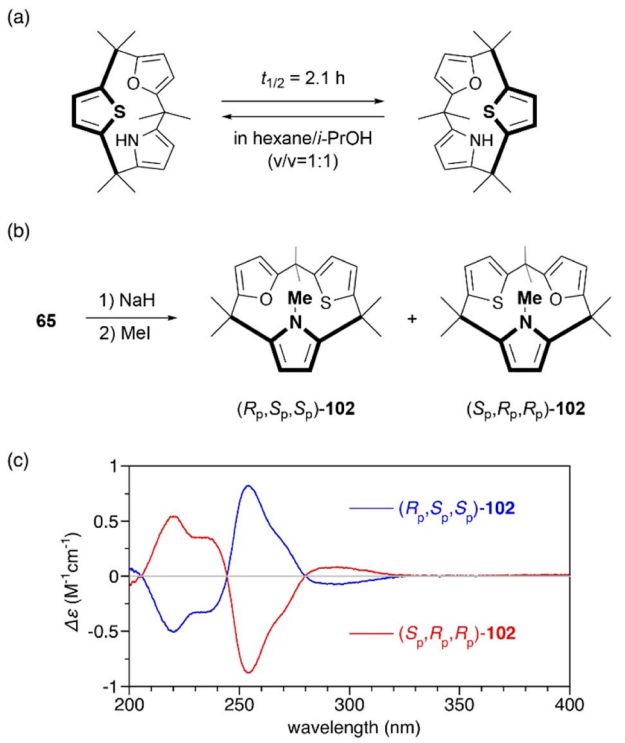

Fig. 12 (a) Racemization of chiral calix[3]pyrrole analogue **65**. (b) *N*-Methylation of **65** to suppresses racemization through ring flipping. (c) CD spectra of **102** in *n*-hexane.

4. Conclusion and future perspectives

Tackling the total synthesis of natural products has led to the development of new synthetic methods.[109–112] Similarly, resolving the various challenges in the synthesis of non-natural contracted porphyrins and calixpyrroles has contributed to the discovery of not only new reactions but also functional chromophores, metal complexes, and supramolecules. Controlling the ring strain during macrocyclization is crucial to obtain contracted porphyrinoids with a macrocyclic ring size smaller than the marginal size of compounds obtained *via* Rothemund–Lindsey protocol. Therefore, unique approaches have been developed, including boron templating, core-modification, and ring tightening. Boron-templated synthesis has led to the discovery of unusual boron-chelation effects in subporphyrins, which allows orthogonal functionalization by axial ligand exchange. Core-modification of the triphyrin(1.1.1) skeleton enables the incorporation of various heteroarenes and additional *meso*-carbon atoms, which provides scaffolds for the generation of their metal complexes. Furthermore, the ring tightening approach provides a rational route to calix[3]pyrroles, leading to the discovery of strain-induced ring expansion reactions.

The ring contraction effects on reactivity, structure, and optical properties have been demonstrated, namely contracted macrocycles have properties that are similar but distinct from those of their parent porphyrinoids. Revealing hidden contraction effects should be a key to advancing this emerging research area. There are still a number of synthetic targets that have not yet been achieved. For example, the synthesis of triphyrin(1.1.0), a corrole-type[113] tripyrrole macrocycle, requires unconventional approaches to overcome the significant increase in ring strain during macrocyclization. Highly contracted macrocycles composed of only two pyrrole units might link the chemistry of porphyrins and cyclophanes, although theoretical calculations have shown an unrealistic increase in their strain energy even with the ring tightening approach.[114] Furthermore, the development of general methods for the removal of boron templates from boron-subporphyrins is of significant interest, as it will expand the coordination chemistry of subporphyrins. As research on non-natural contracted porphyrins and calixpyrroles transitions from the infant stage (synthetic attempts) to the application stage (development of functional molecules), new aspects of porphyrin-related compounds will be uncovered.

Author contributions

Y. I. outlined all the sections, wrote the first draft of the manuscript, and revised subsequent drafts of the manuscript. K. W. and N. N. P. provided input and feedback on each section and contributed to subsequent drafts of the manuscript. K. W. and Y. I. created the original figures.

Conflicts of interest

There are no conflicts to declare.

Acknowledgements

The authors acknowledge support from the JSPS Grant-in-Aid for Scientific Research (B) (No. 22H02058) and the JST FOREST Program (No. JPMJFR211H), of which Y. I. is the principal investigator. The Institute for Chemical Reaction Design and Discovery (ICReDD) was established by World Premier International Research Initiative (WPI), MEXT, Japan. Dedicated to Professor Atsuhiro Osuka on his 70th birthday.

Notes and references

1 L. R. Milgrom, *The Colours of Life: An Introduction to the Chemistry of Porphyrins and Related Compounds*, Oxford University Press, 1997.
2 J. G. Riess, *Chem. Rev.*, 2001, **101**, 2797–2920.
3 J. M. Cole, P. Giulio, O. K. Al Bahri and C. B. Cooper, *Chem. Rev.*, 2019, **119**, 7279–7327.
4 R. Paolesse, S. Nardis, D. Monti, M. Stefanelli and C. D. Natale, *Chem. Rev.*, 2017, **117**, 2517–2583.
5 M. Urbani, M. Grätzel, M. K. Nazeeruddin and T. Torres, *Chem. Rev.*, 2014, **114**, 12330–12396.
6 Y. Zhang, T. Higashino and H. Imahori, *J. Mater. Chem. A*, 2023, **11**, 12659–12680.
7 H. Imahori and M. Akiyama, *J. Porphyrins Phthalocyanines*, 2024, **28**, DOI: 10.1142/S1088424624300015.
8 K. Gopalaiah, *Chem. Rev.*, 2013, **113**, 3248–3296.
9 B. Meunier, *Chem. Rev.*, 1992, **92**, 1411–1456.
10 W. Zhang, W. Lai and R. Cao, *Chem. Rev.*, 2017, **117**, 3717–3797.
11 S. Erbas-Cakmak, D. A. Leigh, C. T. McTernan and A. L. Nussbaumer, *Chem. Rev.*, 2015, **115**, 10081–10206.
12 R. B. Woodward, *Pure Appl. Chem.*, 1968, **17**, 519–547.
13 P. Rothemund, *J. Am. Chem. Soc.*, 1935, **57**, 2010–2011.
14 R. B. Woodward, *Aromaticity: An International Symposium Sheffield, 1966, Special Publication no. 21*, The Chemical Society, London, 1966.
15 T. Tanaka and A. Osuka, *Chem. Rev.*, 2017, **117**, 2584–2640.
16 J. L. Sessler and D. Seidel, *Angew. Chem., Int. Ed.*, 2003, **42**, 5134–5175.
17 T. Sarma and P. K. Panda, *Chem. Rev.*, 2017, **117**, 2785–2838.
18 J. Setsune, Y. Katakami and N. Iizuna, *J. Am. Chem. Soc.*, 1999, **121**, 8957–8958.
19 J. Setsune and S. Maeda, *J. Am. Chem. Soc.*, 2000, **122**, 12405–12406.
20 A. Dondoni and A. Marra, *Chem. Rev.*, 2010, **110**, 4949–4977.
21 J. Szejtli, *Chem. Rev.*, 1998, **98**, 1743.
22 S. J. Barrow, S. Kasera, M. J. Rowland, J. del Barrio and O. A. Scherman, *Chem. Rev.*, 2015, **115**, 12320–12406.
23 A. A. Moshfegh, E. Beladi, L. Radnia, A. S. Hosseini, S. Tofigh and G. H. Hakimelahi, *Helv. Chim. Acta*, 1982, **65**, 1264–1270.
24 D. Ikuta, Y. Hirata, S. Wakamori, Y. Tomabechi, Y. Kawasaki, K. Ikeuchi, T. Hagimori, S. Matsumoto and H. Yamada, *Science*, 2019, **364**, 674–677.
25 J. Kim, I. Jung, S. Kim, E. Lee, J. Kang, S. Sakamoto, K. Yamaguchi and K. Kim, *J. Am. Chem. Soc.*, 2000, **122**, 540–541.
26 Y. Inokuma, J. H. Kwon, T. K. Ahn, M. Yoo, D. Kim and A. Osuka, *Angew. Chem., Int. Ed.*, 2006, **45**, 961–964.
27 C. G. Claessens, D. González-Rodríguez and T. Torres, *Chem. Rev.*, 2002, **102**, 835–853.
28 C. G. Claessens, D. González-Rodríguez, M. S. Rodríguez-Morgade, A. Medina and T. Torres, *Chem. Rev.*, 2014, **114**, 2192–2277.
29 G. Lavarda, G. Labella, M. V. Martinez-Diaz, M. S. Rodríguez-Morgade, A. Osuka and T. Torres, *Chem. Soc. Rev.*, 2022, **51**, 9482–9619.
30 A. Meller and A. Ossko, *Monatsh. Chem.*, 1972, **103**, 150–155.
31 L. Liu, J. Kim, L. Xu, Y. Rao, M. Zhou, B. Yin, J. Oh, D. Kim, A. Osuka and J. Song, *Angew. Chem., Int. Ed.*, 2022, **61**, e202214342.
32 Y. Inaba, Y. Nomata, Y. Ide, J. Pirillo, Y. Hijikata, T. Yoneda, A. Osuka, J. L. Sessler and Y. Inokuma, *J. Am. Chem. Soc.*, 2021, **143**, 12355–12360.
33 P. A. Gale, P. Anzenbecher Jr and J. L. Sessler, *Coord. Chem. Rev.*, 2001, **222**, 57–102.
34 S. K. Kim and J. L. Sessler, *Acc. Chem. Res.*, 2014, **47**, 2525–2536.

35 J. S. Park, E. Karnas, K. Ohkubo, P. Chen, K. M. Kadish, S. Fukuzumi, C. W. Bielawski, T. W. Hundnall, V. M. Lynch and J. L. Sessler, *Science*, 2010, **329**, 1324–1327.
36 I. Saha, J. T. Lee and C.-H. Lee, *Eur. J. Org Chem.*, 2015, 3859–3885.
37 S. Peng, Q. He, G. I. Vargas-Zúñiga, L. Qin, I. Hwang, S. K. Kim, N. J. Heo, C.-H. Lee, R. Dutta and J. L. Sessler, *Chem. Soc. Rev.*, 2020, **49**, 865.
38 D. S. Kim and J. L. Sessler, *Chem. Soc. Rev.*, 2015, **44**, 532–546.
39 F. H. Kohnke, *Eur. J. Org Chem.*, 2020, 4261–4272.
40 Y. Matano, *Org. Biomol. Chem.*, 2023, **21**, 3034–3056.
41 R. K. Sharma, G. Ahuja and I. T. Sidhwani, *Green Chem. Lett. Rev.*, 2009, **2**, 101–105.
42 D. Langerreiter, M. A. Kostiainen, S. Kaabel and E. Anaya-Plaza, *Angew. Chem., Int. Ed.*, 2022, **61**, e202209033.
43 L. Edwards, M. Gouterman and C. B. Rose, *J. Am. Chem. Soc.*, 1976, **98**, 7638–7641.
44 N. Kobayashi, Y. Takeuchi and A. Matsuda, *Angew. Chem., Int. Ed.*, 2007, **46**, 758–760.
45 A. Alder, F. Longo and W. Shergalis, *J. Am. Chem. Soc.*, 1964, **86**, 3145–3149.
46 P. Szarvas, B. Gyori and J. Emri, *Acta Chim. Acad. Sci. Hung.*, 1971, **70**, 1–8.
47 Y. Inokuma, Z. S. Yoon, D. Kim and A. Osuka, *J. Am. Chem. Soc.*, 2007, **129**, 4747–4761.
48 E. Tsurumaki, S. Saito, K. S. Kim, J. M. Lim, Y. Inokuma, D. Kim and A. Osuka, *J. Am. Chem. Soc.*, 2008, **130**, 438–439.
49 M. Kitano, S. Hayashi, T. Tanaka, H. Yorimitsu, N. Aratani and A. Osuka, *Angew. Chem., Int. Ed.*, 2012, **51**, 5593–5597.
50 T. Tanaka, M. Kitano, S. Hayashi, H. Yorimitsu, N. Aratani and A. Osuka, *Org. Lett.*, 2012, **14**, 2694–2697.
51 K. Kise, K. Yoshida, R. Kotani, D. Shimizu and A. Osuka, *Chem.–Eur. J.*, 2018, **24**, 19136–19140.
52 O. I. Koifmana and T. A. Ageeva, *Russ. J. Org. Chem.*, 2022, **58**, 443–479.
53 S. Saito, K. S. Kim, Z. S. Yoon, D. Kim and A. Osuka, *Angew. Chem., Int. Ed.*, 2007, **46**, 5591–5593.
54 R. Sakamoto, S. Saito, S. Shimizu, Y. Inokuma, N. Aratani and A. Osuka, *Chem. Lett.*, 2010, **39**, 439–441.
55 M. S. Rodríguez-Morgade, S. Esperanza, T. Torres and J. Barberá, *Chem.–Eur. J.*, 2005, **11**, 354–360.
56 Z. Li, L. Zhang, Q. Wu, h. Li, Z. Kang, C. Yu, E. Hao and L. Jiao, *J. Am. Chem. Soc.*, 2022, **144**, 6692–6697.
57 Z. Xue, Z. Shen, J. Mack, D. Kuzuhara, H. Yamada, T. Okujima, N. Ono, X. You and N. Kobayashi, *J. Am. Chem. Soc.*, 2008, **130**, 16478–16479.
58 Z. Xue, J. Mack, H. Lu, L. Zhang, X. Z. You, D. Kuzuhara, M. Stillman, H. Yamada, S. Yamauchi, T. N. Kobayashi and Z. Shen, *Chem.–Eur. J.*, 2011, **17**, 4396–4407.
59 S. Ito, N. Ochi, T. Murashima, H. Uno and N. Ono, *Heterocycles*, 2000, **52**, 399–411.
60 K. S. Anju, S. Ramakrishnan and A. Srinivasan, *Org. Lett.*, 2012, **13**, 2498–2501.
61 J. S. Lindsey, *Acc. Chem. Res.*, 2010, **43**, 300–311.
62 D. Kuzuhara, H. Yamada, Z. L. Xue, T. Okujima, S. Mori, Z. Shen and H. Uno, *Chem. Commun.*, 2011, **47**, 722–724.
63 B. S. Kumar, N. N. Pati, K. V. Jovan Jose and P. K. Panda, *Chem. Commun.*, 2020, **56**, 5637–5640.
64 R. Myśliborski, L. Latos-Grażyński, L. Szterenberg and T. Lis, *Angew. Chem., Int. Ed.*, 2006, **45**, 3670–3674.
65 M. Pawlicki, M. Garbicz, L. Szterenberg and L. Latos-Grażyński, *Angew. Chem., Int. Ed.*, 2015, **54**, 1906–1909.
66 D. Kuzuhara, Y. Sakakibara, S. Mori, T. Okujima, H. Uno and H. Yamada, *Angew. Chem., Int. Ed.*, 2013, **52**, 3360–3363.
67 K. Watanabe, K. Shibata, T. Ichino, Y. Ide, T. Yoneda, S. Maeda and Y. Inokuma, *ChemRxiv*, 2024, preprint, DOI: **10.26434/chemrxiv-2024-6nqnq.v1**.
68 S. Maeda, K. Ohno and K. Mororkuma, *Phys. Chem. Chem. Phys.*, 2013, **15**, 3683–3701.
69 C. E. Colwell, T. W. Price, T. Stauch and R. Jasti, *Chem. Sci.*, 2020, **11**, 3923–3930.
70 P. J. Evans, E. R. Darzi and R. Jasti, *Nat. Chem.*, 2014, **6**, 404–408.
71 E. Kayahara, V. Kumar Patel and S. Yamago, *J. Am. Chem. Soc.*, 2014, **136**, 2284–2287.
72 V. Martí-Centelles, M. D. Pandey, M. I. Burguete and S. V. Luis, *Chem. Rev.*, 2015, **115**, 8736–8834.
73 G. Cafeo, F. H. Kohnke, G. L. La Torre, A. J. P. White and D. J. Williams, *Angew. Chem., Int. Ed.*, 2000, **39**, 1496–1498.
74 G. Cafeo, F. H. Kohnke, M. F. Parisi, R. P. Nascone, G. L. La Torre and D. J. Williams, *Org. Lett.*, 2002, **4**, 2695–2697.
75 G. Cafeo, F. H. Kohnke, G. L. La Torre, M. F. Parisi, R. P. Nascone, A. J. P. White and D. J. Williams, *Chem.–Eur. J.*, 2002, **8**, 3148–3156.
76 Y. Manabe, M. Uesaka, T. Yoneda and Y. Inokuma, *J. Org. Chem.*, 2019, **84**, 9957–9964.
77 P. Sarkar, Y. Inaba, H. Shirakura, T. Yoneda and Y. Inokuma, *Org. Biomol. Chem.*, 2020, **18**, 3297–3302.
78 N. Ozawa, K. I. Shivakumar, M. Murugavel, Y. Inaba, T. Yoneda, Y. Ide, J. Pirillo, Y. Hijikata and Y. Inokuma, *Chem. Commun.*, 2022, **58**, 2971–2974.
79 M. Uesaka, Y. Saito, S. Yoshioka, Y. Domoto, M. Fujita and Y. Inokuma, *Commun. Chem.*, 2018, **1**, 23.
80 Y. Inaba, Y. Kakibayashi, Y. Ide, J. Pirillo, Y. Hijikata, T. Yoneda and Y. Inokuma, *Chem.–Eur. J.*, 2022, **28**, e202200056.
81 Y. Inaba, J. Yang, Y. Kakibayashi, T. Yoneda, Y. Ide, Y. Hijikata, J. Pirillo, R. Saha, J. L. Sessler and Y. Inokuma, *Angew. Chem., Int. Ed.*, 2023, **62**, e202301460.
82 E. Tsurumaki, S. Hayashi, F. S. Tham, C. A. Reed and A. Osuka, *J. Am. Chem. Soc.*, 2011, **133**, 11956–11959.
83 T. Kato, F. S. Tham, P. D. W. Boyd and C. A. Reed, *Heteroat. Chem.*, 2006, **17**, 209–216.
84 Y. Tobe, K. Ueda, K. Kakiuchi, Y. Odaira, Y. Kai and N. Kasai, *Tetrahedron*, 1986, **42**, 1851–1858.
85 P. Rothemund and A. Menotti, *J. Am. Chem. Soc.*, 1948, **70**, 1808–1812.
86 K. M. Kadish, E. C. Van and G. Royal, *The Porphyrin Handbook*, ed. K. M. Kadish, K. M. Smith and R. Guilard, Academic Press, San Diego, 2000, vol. 8, pp. 1–219.
87 Y. Inokuma, S. Easwaramoorthi, Z. S. Yoon, D. Kim and A. Osuka, *J. Am. Chem. Soc.*, 2008, **130**, 12234–12235.

88 C. Ngaojampa, S. Namuangruk, Y. Surakhot, V. Promarak, S. Jungsuttiwong and N. Kungwan, *Comput. Theor. Chem.*, 2015, **1062**, 1–10.
89 Y. Inokuma, S. Easwaramoorthi, S. Y. Jang, K. S. Kim, D. Kim and A. Osuka, *Angew. Chem., Int. Ed.*, 2008, **47**, 4840–4843.
90 K. Watanabe, R. Saha, Y. Inaba, Y. Manabe, T. Yoneda, Y. Ide, Y. Hijikata and Y. Inokuma, *J. Porphyrins Phthalocyanines*, 2023, **27**, 157–163.
91 S. Shimizu, A. Matsuda and N. Kobayashi, *Inorg. Chem.*, 2009, **48**, 7885–7890.
92 S. Saga, S. Hayashi, K. Yoshida, E. Tsurumaki, P. Kim, Y. M. Sung, J. Sung, T. Tanaka, D. Kim and A. Osuka, *Chem.–Eur. J.*, 2013, **19**, 11158–11161.
93 E. Tsurumaki, J. Sung, D. Kim and A. Osuka, *J. Am. Chem. Soc.*, 2015, **137**, 1056–1059.
94 E. Tsurumaki, J. Sung, D. Kim and A. Osuka, *Angew. Chem., Int. Ed.*, 2016, **55**, 2596–2599.
95 D. Kuzuhara, Z. Xue, S. Mori, T. Okujima, H. Uno, N. Aratani and H. Yamada, *Chem. Commun.*, 2013, **49**, 8955–8957.
96 Z. Xue, D. Kuzuhara, S. Ikeda, Y. Sakakibara, K. Ohkubo, N. Aratani, T. Okujima, H. Uno, S. Fukuzumi and H. Yamada, *Angew. Chem., Int. Ed.*, 2013, **52**, 7306–7309.
97 Z. Xue, Y. Wang, J. Mack, Y. Fang, Z. Ou, W. Zhu and K. M. Kadish, *Inorg. Chem.*, 2015, **54**, 11852–11858.
98 Z. Xue, D. Kuzuhara, S. Ikeda, T. Okujima, S. Mori, H. Uno and H. Yamada, *Inorg. Chem.*, 2013, **52**, 1688–1690.
99 M. C. Stuparu, *Acc. Chem. Res.*, 2021, **54**, 2858–2870.
100 A. Salazar, M. Moreno-Simoni, S. Kumar, J. Labella, T. Torres and G. de la Torre, *Angew. Chem., Int. Ed.*, 2023, **62**, e202311255.
101 K. Yoshida and A. Osuka, *Chem.–Asian J.*, 2015, **10**, 1526–1534.
102 K. Yoshida and A. Osuka, *Chem.–Eur. J.*, 2016, **22**, 9396–9403.
103 Y. Inokuma and A. Osuka, *Chem. Commun.*, 2007, 2938–2940.
104 D. Shimizu, J. Oh, K. Furukawa, D. Kim and A. Osuka, *Angew. Chem., Int. Ed.*, 2015, **54**, 6613–6617.
105 P. A. Gale, J. L. Sessler, V. Král and V. Lynch, *J. Am. Chem. Soc.*, 1996, **118**, 5140–5141.
106 R. Saha, J. Pirillo, Y. Ide, Y. Inokuma and Y. Hijikata, *Theor. Chem. Acc.*, 2023, **50**, 142.
107 V. Böhmer, D. Kraft and M. Tabatabai, *J. Inclusion Phenom. Mol. Recognit. Chem.*, 1994, **19**, 17–39.
108 M. Kitamura, S. Shirakawa and M. Maruoka, *Angew. Chem., Int. Ed.*, 2005, **44**, 1549–1551.
109 J. ApSimon, *Total Synthesis of Natural Products*, John Wiley & Sons, Inc., 1973.
110 K. C. Nicolaou, S. A. Snyder, T. Montagnon and G. Vassilikogiannakis, *Angew. Chem., Int. Ed.*, 2002, **41**, 1668–1698.
111 W. R. Gutekunst and P. S. Baran, *Chem. Soc. Rev.*, 2011, **40**, 1976–1991.
112 B. M. Trost and M. L. Crawley, *Chem. Rev.*, 2003, **103**, 2921–2943.
113 R. Orłowski, D. Gryko and D. T. Gryko, *Chem. Rev.*, 2017, **117**, 3102–3137.
114 T. Sano, Y. Sun, T. Mukai, Y. Inaba, T. Yoneda, Y. Ide, J. Pirillo, Y. Hijikata and Y. Inokuma, *J. Porphyrins Phthalocyanines*, 2023, **27**, 1067–1073.